frontiers in Marine Science

ORIGINAL RESEARCH
published: 09 June 2020
doi: 10.3389/fmars.2020.00393

Drivers of Megabenthic Community Structure in One of the World's Deepest Silled-Fjords, Sognefjord (Western Norway)

Heidi K. Meyer[1], Emyr M. Roberts[1], Furu Mienis[2] and Hans T. Rapp[1,3†]*

[1] Department of Biological Sciences and K.G. Jebsen Centre for Deep-Sea Research, University of Bergen, Bergen, Norway, [2] Department of Ocean Systems, Royal Netherlands Institute for Sea Research and Utrecht University, Den Burg, Netherlands, [3] NORCE, Norwegian Research Centre, NORCE Environment, Bergen, Norway

The Sognefjord is the longest (205 km) and deepest (1308 m) fjord in Norway, and the second-longest in the world. Coast-fjord exchange in Sognefjord is limited by a seaward sill at 170 m water depth, which causes a clear stratification between water masses as the dense oxygen-poor basin water mixes slowly with the well-oxygenated water directly above from the coastal ocean. Due to the homogeneity and limited variability in the deep-water, the deep slopes of Sognefjord represent the ideal setting to study how abiotic factors influence the deep-water benthic community structure. During the summer of 2017, two remotely operated vehicle (ROV) video transects were performed to compare the megabenthic community behind the sill (water depth: 1230 to 55 m; transect length: 1.39 km; distance from sill: ∼17 km) and within the central fjord (water depth: 1155–85 m; transect length: 2.43 km; distance from sill: ∼79 km). Accompanying conductivity–temperature–depth (CTD) deployments were made to measure the *in situ* abiotic factors and nutrient concentrations at each transect location, while the substrate characteristics (percent cover of soft and hard exposed substrate) were documented from the video footage. Here, Sognefjord's megabenthic community composition, distribution, and species richness were analyzed in relation to abiotic factors (e.g., depth, salinity, dissolved oxygen, chlorophyll *a* concentration, and percent cover of hard and soft substrata) within the fjord. Basin communities were homogeneous and characterized by sponges, echinoderms, and crustaceans, whereas the shallower regions were dominated by mobile scavengers. Contrary to other fjord-based studies, species richness and diversity were stable in the fjord basin and decreased with proximity to the sill, decreasing water depth, and at the boundary between intermediate and basin water. The findings demonstrate that highly stratified fjords support stable communities in their basins; however, further research is needed to investigate the influence water mass dynamics have on silled-fjord megafauna communities.

Keywords: fjord fauna, glass sponges, megafauna, Sognefjord, Norwegian fjords, remotely operated vehicles, extreme habitats

OPEN ACCESS

Edited by:
Thomas Wernberg, University of Western Australia, Australia

Reviewed by:
Giorgio Bavestrello, University of Genoa, Italy
Torstein Pedersen, UiT The Arctic University of Norway, Norway

****Correspondence:***
Heidi K. Meyer
Heidi.Meyer@uib.no

† Deceased

Specialty section:
This article was submitted to Global Change and the Future Ocean, a section of the journal Frontiers in Marine Science

Received: *13 December 2019*
Accepted: *07 May 2020*
Published: *09 June 2020*

Citation:
Meyer HK, Roberts EM, Mienis F and Rapp HT (2020) Drivers of Megabenthic Community Structure in One of the World's Deepest Silled-Fjords, Sognefjord (Western Norway). Front. Mar. Sci. 7:393. doi: 10.3389/fmars.2020.00393

INTRODUCTION

Deep fjords are valuable study areas because they allow easy access to habitats that share similarities with continental shelf or deep-sea communities found in the open ocean (Bernd, 1993; Sweetman and Witte, 2008; Storesund et al., 2017). Their accessibility allows researchers to study the influence of abiotic factors on the shelf or deep-sea community ecology whilst reducing the limitations of cost and transportation that is often problematic for deep-sea research.

It is well documented that fjord communities are influenced by both the coast-fjord and/or depth gradients (Buhl-Mortensen and Høisaeter, 1993; Holte et al., 2004; Włodarska-Kowalczuk and Pearson, 2004; Storesund et al., 2017; Molina et al., 2019). The interaction between the ocean water and the fjord system helps carry seawater into the fjord, which aids in the distribution of fauna, organic nutrients, and inorganic material (Buhl-Mortensen and Høisaeter, 1993; Holte et al., 2004). However, within silled-fjords, the exchange of seawater between the coastal and fjord systems is reduced. The sill height, fjord topography, and freshwater input influences the transport of nutrients, pelagic larvae, organic matter, and dissolved oxygen, where benthic communities toward the inner fjord regions are negatively impacted due to the decreased access to resources (e.g., dissolved oxygen, organic carbon, nutrients) (Buhl-Mortensen and Høisaeter, 1993; Blanchard et al., 2010; Storesund et al., 2017). Density stratification between upper and bottom water masses is often observed and the inner basin(s) below the sill depth becomes isolated from the adjacent coastal system. This stratification leads to relatively stable temperatures and salinities within the basins (Renaud et al., 2007; Drewnik et al., 2016; Molina et al., 2019). With limited mixing within the water column, dissolved oxygen levels tend to decrease with depth, distance from the sill, and over time until a renewal event occurs, whereby more oxygenated ocean water mixes with fjord water. In general, faunal diversity and species richness is seen to decrease with increasing distance from the coastal regions and increasing water depth (Buhl-Mortensen and Høisaeter, 1993; Holte et al., 2004; Molina et al., 2019).

Deep-water stagnation is thought have a major influence on fjord basin communities, where lower oxygen concentrations can negatively impact the community structure and species composition (Blanchard et al., 2010; Molina et al., 2019), resulting in lower species richness with lower oxygen levels (Buhl-Mortensen and Høisaeter, 1993). In periods of hypoxic and anoxic conditions, where the oxygen concentration is <2.1 mL L^{-1}, defaunation of macrofauna and changes in faunal assemblages have been observed within the basin (Holte et al., 2005; Molina et al., 2019). In extreme cases of deoxygenation and strong stratification, a rise of acidification within fjord basins can occur (Jantzen et al., 2013), particularly if water exchange with adjacent coastal systems is insufficient.

Sognefjord is Norway's longest and deepest fjord. It is host to numerous towns and villages and has become a sought-out destination for many cruise ships, where thousands of tourists visit the fjord each year. There is concern on how these anthropogenic influences impact the fjord's marine habitat (Manzetti and Stenersen, 2010). Numerous studies in recent years have been conducted primarily on the microbial community (Poremba and Jeskulke, 1995; Storesund et al., 2017) or the influence of phytodetrital pulses on the macrofaunal community (Witte et al., 2003). Despite the accessibility of Sognefjord, the epibenthic megafauna community has been poorly studied, especially in recent years (Bernd, 1993). Bernd (1993) found that the central fjord and shallower adjacent side-fjord, Høyangsfjord, were primarily dominated by soft-bottom dwelling burrowing decapods (*Munida sarsi* and *Munida tenuimana*), holothurians (*Bathyplotes natans* and *Parastichopus tremulus*), and anthozoans. Høyangsfjord was found to have a lower megafaunal density compared to the main fjord. However, besides depth and general observations of substrate type, no thorough analysis was conducted on the influence of abiotic variables on the megafaunal community, especially over a horizontal or vertical gradient. In recent years several expeditions by the University of Bergen and the Institute for Marine Research in Norway, have taken place in the main- as well as the side-fjords, and knowledge about the fauna and benthic communities in Sognefjord is expected to increase rapidly when new data are made available over the coming years (Buhl-Mortensen et al., 2017; H. Glenner, personal communication).

In the present study, we used visual data collected with the remotely operated vehicle (ROV) *AEgir 6000* to investigate the benthic megafaunal community diversity and distribution in Sognefjord and the influence of abiotic variables on the community structure at two locations in the fjord. It is expected that the communities would be less diverse and dense with increasing distance from the sill due to the extremely stable conditions identified by Storesund et al. (2017) (see the section "Study Area" for site description). For this study, we had three main objectives: (1) characterize the benthic community structure based on their depth and distance from the sill, (2) detect any response in community structure and diversity to changes in water mass characteristics above and below the sill, and (3) examine the relationships between environmental conditions and community composition and diversity (using generalized linear models, or GLMs).

MATERIALS AND METHODS

Study Area

Sognefjord is located on the western Norwegian coast, extends to about 205 km and has a maximum water depth of 1308 m (Poremba and Jeskulke, 1995; Storesund et al., 2017). The fjord has a 3-layer water column structure (Svendsen, 2006; Storesund et al., 2017): the top layer is brackish water (salinity $\leq$ 33 psu), formed by the mixture of freshwater runoff and seawater, and moves out of the fjord; the intermediate layer (salinity between 33 and 35 psu) is well-oxygenated, owing to exchanges with the Norwegian Coastal Current above the sill depth, and hosts compensatory flows that may be in-fjord or out-fjord; and the bottom, or basin, water below the sill depth (salinity $>$ 35 psu after deep-water renewal) originates from Atlantic water and becomes gradually less dense between renewal events because

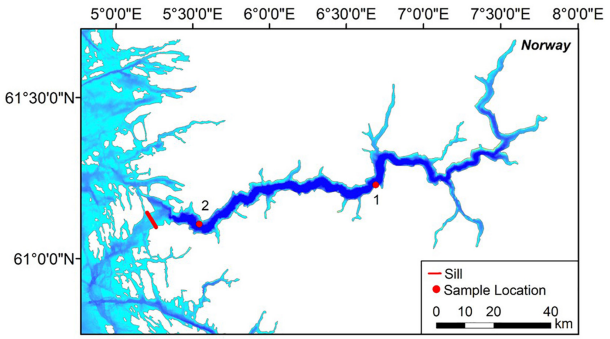

FIGURE 1 | Location of the two *AEgir 6000* transects in Sognefjord, Norway. Digital bathymetry with a resolution of 1/16 × 1/16 arc min was extracted from EMODnet Bathymetry Consortium (2018). ArcGIS (version 10.4; Environmental Systems Research Institute [ESRI], 2016) was used to map the transects.

of diffusion and mixing with the layer above, driven by tidal forcing. Whilst the shallow sill (170 m) at the mouth of the fjord allows for some exchange of water between the fjord system and the adjacent coastal water, the mixing is fairly reduced and strong stratification occurs because of the influx of terrestrial runoff (Storesund et al., 2017). Renewal of the basin water occurs approximately every 8 years (Buhl-Mortensen et al., 2020).

Conditions within the fjord basin below sill depth are fairly stable and homogeneous. Water temperature is consistently around 7.4°C and the salinity is generally greater than 35.0 psu (Witte et al., 2003; Storesund et al., 2017). Oxygen concentrations have been found to decrease with increasing distance from the sill and with depth, where Storesund et al. (2017) found the inner fjord and lower basin water to have oxygen concentrations below 4.5 mL L^{-1} in May and November 2012.

Data Collection

Two video transects were performed with the work-class ROV *Ægir 6000* in Sognefjord in July 2017 during a SponGES cruise with the R.V. *G.O. Sars* (**Figure 1**). Dive 1 (D1) was conducted within the central fjord (1155 – 85 m; 61° 6′ N, 6° 39′ E) and Dive 2 (D2) was located near the sill (1230 – 55 m; 61° 3′ N, 5° 22′ E), respectively. D1 and D2 had approximate transect lengths of 2.43 km and 1.39 km, and were located approximately 79 km and 17 km away from the sill, respectively. The approximate fjord side slopes for D1 and D2 are 43° and 44° inclined to the horizontal plane. Physical samples were collected by the ROV during the transects to help confirm identifications of fauna.

One ship-based conductivity–temperature–depth (CTD) sensor package cast was conducted for each transect to profile temperature (°C), salinity (psu), dissolved oxygen (mL L^{-1}) and chlorophyll *a* concentration (μg L^{-1}) throughout the water column. The bottom depths of the CTD casts corresponding to D1 and D2 were 1017 m and 1223 m, respectively. In addition, water samples were collected (using a rosette water sampler, on which the CTD package was mounted) from the different water masses for nutrient analysis. From the video footage, the percent cover of exposed hard substrate and soft sediment was estimated for each image analyzed.

Nutrient Content Analysis

Seawater samples for the analysis of inorganic dissolved nutrients (Si, PO_4, NH_4, NO_3, and NO_2) were collected with the CTD-rosette from selected depths. Sample depths were selected based on the profile of the CTD downcast, whereby samples were collected from five different depths. Subsamples were collected in 50 mL syringes, which were rinsed three times with water from the niskin bottles of the CTD rosette before being filled. After sampling on deck, samples were filtered through 0.2 μm filters and instantly sub-sampled into two vials, one of which was used for samples of ortho-phosphate (PO_4), ammonium (NH_4), nitrate (NO_3), and nitrite (NO_2), stored at −20°C and the other for silicate (Si), stored at 4°C. Nutrients were analyzed at NIOZ with a QuAAtro Gas Segmented Continuous Flow Analyzer. Measurements were made simultaneously on four channels for PO_4 (Murphy and Riley, 1962), NH_4 (Helder and De Vries, 1979), NO_2, and NO_3 (Grasshoff et al., 1983). Si was measured during a separate run (Strickland and Parsons, 1968). All measurements were calibrated with standards diluted in low nutrient seawater. For a detailed description of the sampling procedure we refer to Roberts et al. (2018).

Video Annotation

Still images were extracted from the videos approximately every 30 s to ensure there was no spatial overlap between images during analysis. Due to fluctuations in ROV altitude and changes in turbidity or topography, some areas of the transects were not suitable for analysis. Images were excluded if they contained any of the following characteristics: (1) image area obscured by part of the ROV or suspended material, (2) ROV was collecting physical specimens, (3) ROV was too far from the substrate (>10 m), (4) camera angle was not seabed-facing, (5) image contained poor light visibility, (6) image was blurred, and (7) overlapping image area. Videos were rescanned during image annotation to help identify individuals that were difficult to decipher in the stills alone, and in some cases, new stills were extracted if a more suitable image was present ±5 s from the original still. This was mostly the case for images that were blurred or contained poor light visibility and more suitable images of the same area were available within 5 s of the original image extracted. Parallel lasers of known separation (which project spots onto the seabed in order to determine image scale) were only active for the first hour of D1. It was therefore not possible to determine area (m^2) and density (individuals m^{-2}) for the survey and megafauna were enumerated based on individuals per image.

ImageJ (version 1.52) was used to annotate the extracted imagery. A virtual grid with 496 cells was overlaid on each image in ImageJ. The grid size was selected because the cells completely overlapped the images. Percent cover of substrate type was estimated by counting the number of grid cells that contained that particular substrate type, then calculating the percentage of the total number of grid cells represented by that value. The grid resolution was selected such that the cells were small enough to minimize the number containing multiple substrate types as

a proportion of total number of cells (and thereby increase the precision in the percent cover estimates) and large enough that the gridlines were not so dense as to obscure the fauna present in the image. In cases where cells contained multiple substrate types, the cell was characterized as the substrate that covered more than half of the cell. All epibenthic megafauna individuals that were easily visible within the imagery were counted and identified to the lowest taxonomic level. Due to fluctuations in altitude during video transects, some fauna had to be identified based on gross morphology (e.g., white sponge 1, yellow sponge 2, etc.). Taxa were classified as rare if represented by three or less individuals.

Statistical Analysis

Data Preparation

Based on the description of the Sognefjord water mass structure by Storesund et al. (2017), the biotic and abiotic data were assigned to three depth zones to identify any depth-related changes in the benthic community structure: "Above Sill" ($\leq$170 m), "Intermediate" (>170 to $\leq$300 m), and "Basin" (>300 m). No data from the surface brackish top-layer (1–10 m) was included. Due to differences in sampling frequency between the CTD profiling and image annotation, the abiotic variables were interpolated at 10 m depth intervals in Rstudio (version 1.2.5; RStudio Team, 2019). Nutrient composition was sampled with low frequency and was thereby excluded from statistical analysis. The megafauna abundances were summed into 10 m depth intervals. To account for missing data in the biotic dataset, certain depth intervals were removed from the abiotic dataset prior to statistical analysis. All multivariate statistical analysis was conducted in Primer (version 7) unless otherwise specified.

Environmental Variables

The environmental variables of D1 (central) and D2 (near-sill) were plotted against each other (e.g., temperatures from D1 vs. temperatures, at corresponding depths, from D2) to identify any notable differences in abiotic conditions between dives (**Supplementary Figure S1**). Furthermore, a correlation matrix was generated in Rstudio with package "corrplot" (version 0.84; Wei and Simko, 2017) to identify which abiotic variables were correlated (**Supplementary Figure S2**). Temperature had a strong negative correlation with salinity and positive correlation with dissolved oxygen (rho > 0.9), and was thereby dropped from further analysis. While depth was significantly correlated with the majority of the abiotic variables (p-value < 0.05) and had a moderately strong positive correlation with salinity and negative correlation with dissolved oxygen (rho > 0.7), it was selected to remain since it often acts as a proxy for other abiotic variables that were not measured in the present study. The remaining variables were normalized in Primer prior to multivariate analysis due to the different units used for each variable. A principal component analysis (PCA) of the selected abiotic variables was used to examine the environmental conditions within each depth zone per dive.

Community Composition and Diversity

Due to the lack of lasers throughout most of the dives, the abundances were converted to presence-absence data. A Sørensen similarity matrix between the two dives was calculated on the presence-absence dataset. Non-metric multidimensional scaling (nMDS) plots were constructed for each dive to identify differences between the community structure within each depth zone. An analysis of similarities (ANOSIM) was generated to identify significant differences between the depth zones and dives. SIMPER was used to determine which taxa were considered indicator organisms for each depth zone.

Diversity indices such as species richness and Shannon-Wiener diversity were calculated from the megafauna presence-absence data for the depth zones in both dives to compare the changes in species richness and diversity over the vertical and horizontal gradients. In SPSS (version 25), a Levene's test of homogeneity of variances was used to determine if the diversity indices were homogeneous prior to running a one-way analysis of variance (ANOVA) to determine if there were significant differences for each index. A Tukey honestly significant difference (HSD) *post hoc* test on the diversity indices was used to identify which depth zones were significantly different for each dive.

To examine which environmental variables best explained the variance in species richness and Shannon-Wiener diversity indices, GLMs were generated in Rstudio. The residual deviance was larger than the residual degrees of freedom, therefore a quasi-Poisson error was fitted to the GLMs to account for overdispersion (Zuur et al., 2009). Depth, salinity, dissolved oxygen, chlorophyll *a*, percent cover of exposed hard substrate and soft sediment were included in the GLMs.

RESULTS

Environmental Conditions

In general, the water was slightly warmer, more saline, and more oxygenated in the water column below the sill at D2 (near-sill), relative to the same depths in D1 (central). The top layer of water was made up of warm brackish water (**Figure 2**), and a sub-surface chlorophyll maximum occurred at the halocline between the brackish surface water and intermediate water (approximately at 20 to 30 m). At approximately 80 to 100 m, dissolved oxygen decreased. Dissolved oxygen levels recovered in the intermediate water just below the sill depth. There was a gradual transition between the intermediate water mass and basin water until about 300 m, where a drop in temperature and dissolved oxygen levels occurred. The basin water was fairly homogeneous and there was not much difference in the water properties between the dives, where temperature was around 7.5°C, salinity at 35.06 psu, and dissolved oxygen around 4.2 mL L^{-1}. D1 was frequently covered in soft sediment with exposed hard substrate patches throughout the transect, whereas D2 had distinct regions of solely soft sediment (e.g., bottom of fjord basin) and exposed hard substrate (e.g., along slopes and cliffs). Within the Intermediate Zone, small boulders and rocks became more frequent, and the sediment type became more coarse.

Inorganic nutrient concentrations increased with depth (**Table 1**), showing highest concentrations below 450 m water depth, while lowest concentrations were measured in surface

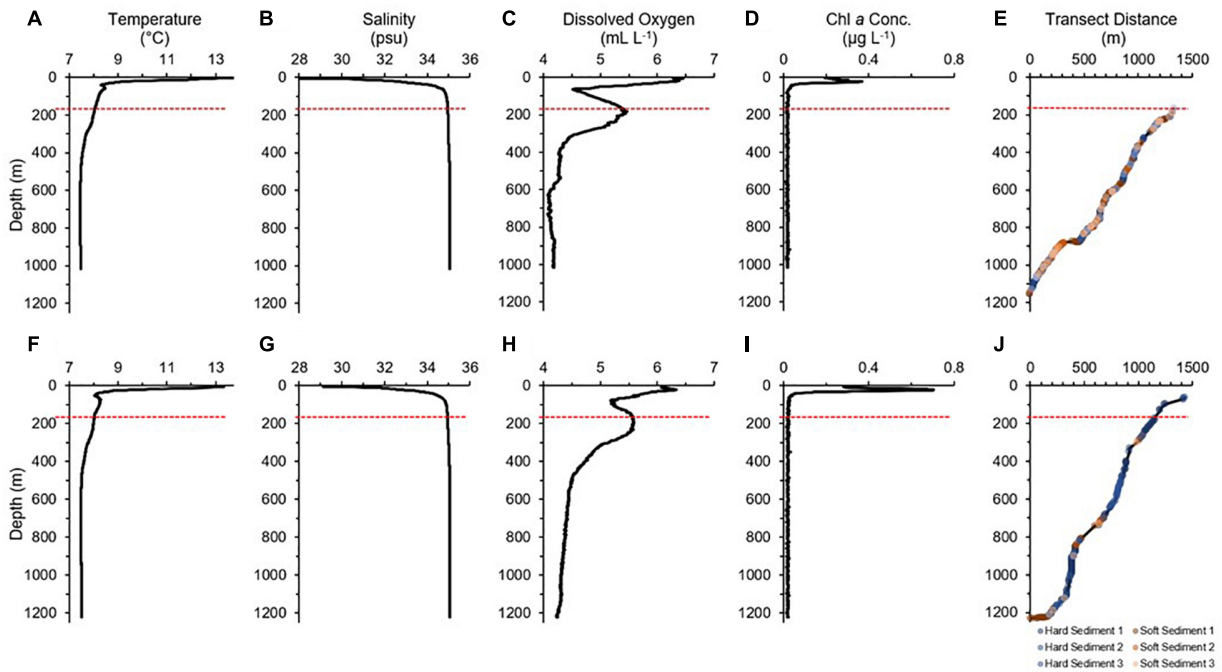

FIGURE 2 | CTD profiles and substrate type for Dive 1 **(A–E)** and Dive 2 **(F–J)** in Sognefjord, Norway. Red dashed line indicates the approximate sill depth (170 m). In **(E,J)**, sediment type 1 to 3 correspond with percent cover, where 1 = 100–91%; 2 = 90–71%; 3 = 70–51%.

TABLE 1 | Concentration of nutrients over depth for Dive 1 (central) and Dive 2 (near-sill) in Sognefjord, Norway.

Dive	*Depth (m)*	*Si* (µmol L(1L-1))	PO_4 ($\mu mol\ L^{-1}$)	NH_4 ($\mu mol\ L^{-1}$)	NO_3 ($\mu mol\ L^{-1}$)	NO_2 ($\mu mol\ L^{-1}$)
1	1028	16.67	1.158	0.202	14.87	0.034
	799	16.85	1.161	0.139	15.05	0.017
	500	14.63	1.114	0.135	14.95	0.019
	150	6.223	0.778	0.153	11.11	0.108
	6	0.153	0.046	0.139	0.135	0.066
2	1237	16.78	1.144	0.221	14.41	0.077
	800	14.52	1.091	0.173	14.39	0.028
	500	13.49	1.07	0.172	14.04	0.034
	150	5.46	0.726	0.112	10.48	0.021
	10	0.097	0.033	0.119	0.073	0.036

waters at both sites. Nutrient concentrations did not show large differences between the two sites.

In D1, from the suspended particulates observed in the video footage, predominately vertical settling appeared to occur. In these regions, sessile fauna and vertical rock walls were covered with a fine layer of particulate matter. However, D2 had higher observed turbidity throughout the dive compared to D1, with the settling of particulate matter apparent and some evidence of horizontal flow based on the position of the feeding apparatus of filter feeders and particulate direction changes.

In the PCA ordination, the first two principal components (PC) represented approximately 76% of the environmental variability within the two dives combined (47.1% and 28.6% for PC1 and PC2, respectively) (**Figure 3**). The PCA ordination showed that the images within the Basin Zones of both D1 and D2 were clearly distinguishable from the Intermediate and Above Sill Zones along the axes of PC1 and PC2. Dissolved oxygen (Eigenvector = 0.503), salinity (Eigenvector = −0.498), and depth (Eigenvector = −0.490) had the strongest influence on PC1. Percent cover of soft sediment (Eigenvector = −0.623) and exposed hard substrate (Eigenvector = 0.613) most strongly influenced PC2.

Sognefjord Megafauna Composition

In total, D1 had 79 taxa with a total of 11557 individuals and D2 had 89 taxa with a total of 10615 individuals (**Table 2**). After rare taxa were excluded from the dataset, there was a total of 22105 individuals and 72 taxa identified within 511 images, where D1 had 11528 individuals and 57 taxa and D2 had 10577 individuals and 63 taxa. Porifera made up the majority of the taxa (24),

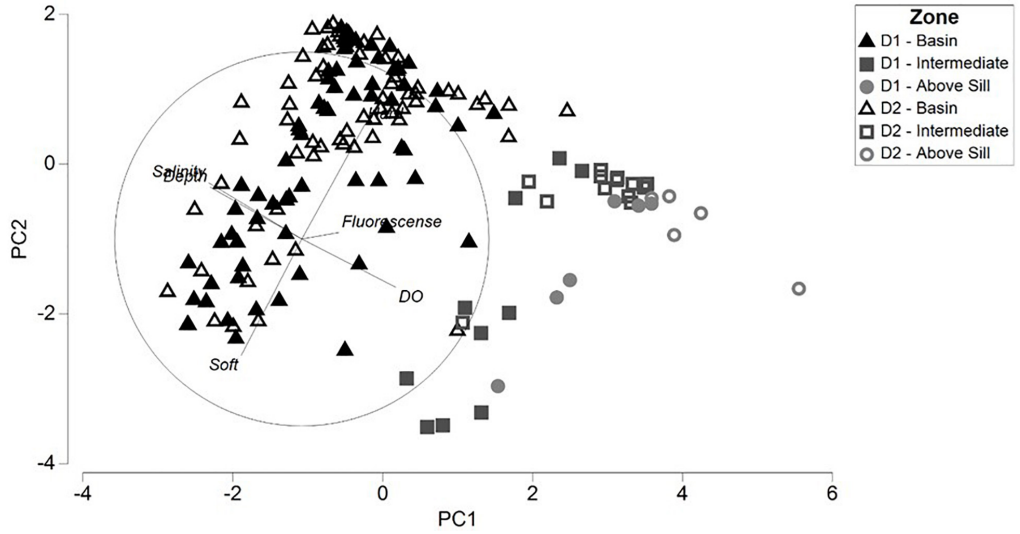

FIGURE 3 | Principal component plot of the abiotic variables for the depth zones within Dive 1 (closed) and Dive 2 (open), with the direction of the respective abiotic variables and their component score influence.

followed by Echinodermata (16), and Cnidaria (10). The Above Sill Zone for both D1 and D2 had the lowest total abundances and number of species compared to the other zones.

The top 10 most abundant taxa for D1 were White Encrusting Sponge 1, *Psolus squamatus* (O.F. Müller, 1776), *Hymedesmia* sp., Brachiopoda 1, *Munida tenuimana* Sars, 1872, *Gracilechinus acutus* (Lamarck, 1816), *Polymastia nivea* (Hansen, 1885), *Gracilechinus elegans* (Düben & Koren, 1844), Yellow Encrusting Sponge 1, and *Stylocordyla borealis* (Lovén, 1868). For D2, the top 10 most abundant taxa were the White Encrusting Sponge 1, Echinoidea 1, *P. squamatus*, *Hymedesmia* sp., *G. acutus*, *M. tenuimana*, Yellow Encrusting Sponge 1, *G. elegans*, *Acesta excavata* (Fabricius, 1779), and *Phakellia* spp.

Community Trends and Observations

Within the Basin Zone, exposed hard substrate was often covered with polychaete tubes, the bivalve *A. excavata*, cnidarians, and encrusting sponges (**Figure 4**). *Acesta excavata* was present in high densities when observed on vertical rocky walls, often with juveniles and dense accumulations of encrusting polychaetes nearby. The octocoral *Anthomastus grandiflorus* (Verril, 1878) (**Figure 4b**) and large glass sponges *Asconema* aff. *foliatum* (Fristedt, 1887) (**Figure 4e**) occurred only on vertical rock walls. In D1, *A.* aff. *foliatum* was covered by a fine layer of suspended particulate matter (**Figure 4e**).

Soft bottom areas were characterized by the enigmatic asteroid *Hymenodiscus coronata* (Sars, 1871), *M. tenuimana*, *Bathyplotes natans* (Sars, 1868), *Mesothuria intestinalis* (Ascanius, 1805), *Psilaster andromeda* (Müller & Troschel, 1842), small patches of *Kophobelemnon stelliferum* (Müller, 1776) and carnivorous sponges, and in rare cases, *Virgularia mirabilis* (Müller, 1776). Signs of lebensspuren such as burrows containing *M. tenuimana* within or nearby were observed throughout both dives (**Figures 4n,p**).

In regions with mixed substrate types (e.g., exposed hard substrate and soft sediment), *Psolus squamatus* was often observed concentrated at breaks in the slope or protruding surfaces. *Phakellia* spp., *Phakellia ventilabrum* (Linnaeus, 1767), and *Axinella infundibuliformis* (Linnaeus, 1759) were commonly positioned along slopes, aligned with the direction of observed horizontal particle flow (**Figure 4m**). Large anemones like *Bolocera tuediae* (Johnston, 1832) were observed residing on exposed hard substrate walls with soft sediment surrounding the substrate.

In the Intermediate and Above Sill Zone of D2, it should also be noted that there was a sudden occurrence of Echinoidea 1 in large quantities (max. 859 individuals per image) from 240 m to 60 m water depth (**Figure 4u**). For D2, the Above Sill Zone had a higher proportion of echinoderms present (**Figures 4v,y**). Numerous fish species, including *Chimaera monstrosa* (Linnaeus, 1758), *Sebastes viviparus* (Krøyer, 1845) (**Figure 4v**), and *Coryphaenoides rupestris* (Gunnerus, 1765), were observed within the upper regions of D1 and D2. Anthropogenic waste was found in the D1 Above Sill Zone (**Figure 4w**).

Community Structure

The community composition of the non-rare taxa showed significant differences between the depth zones and dives (ANOSIM Global R: 0.261, $p = 0.001$) (**Figure 5**). For D1, the nMDS plots and pairwise ANOSIM test indicated that the Basin and Intermediate Zones shared a similar community composition ($p > 0.05$). All other zones showed significant differences in community composition.

The SIMPER analysis revealed that for both dives, all zones except for D2-Above Sill had *P. squamatus*, *Hymedesmia* sp., and White Encrusting Sponge 1 within the top five contributing taxa (**Table 3**). Taxa from the Echinodermata were more common in D2 than D1. For both dives, the Basin and Above Sill

TABLE 2 | The presence (x) of all megafauna within each depth zone for Dive 1 (left) and Dive 2 (right) in Sognefjord, Norway.

				D1				*D2*			
Phylum	***Class (subclass*)***	***Taxon***	**Figure 4 *plate #***	***Basin***	***Intermediate***	***Above sill***	***Total %***	***Basin***	***Intermediate***	***Above sill***	***Total %***
Annelida	Echiura*	*Bonellia viridis* (Rolando, 1822)*	j	x			0.03				
		Maxmuelleria faex (Selenka, 1885)		x			0.17	x	x		0.16
	Sedentaria*	Serpulidae 1		x	x	x	0.36	x			0.22
		Serpulidae 2**	g					x			0.05
		Serpulidae 3**						x			0.01
	Undetermined	**Polychaeta 1***		x			0.03				
Arthropoda	Malacostraca	*Munida tenuimana* Sars, 1872	b, n, o, p	x	x		3.89	x			3.16
		Decapod 1	g	x	x		0.43	x			0.24
		Decapod 2		x			0.09		x		0.01
		Decapod 3**						x	x		0.21
		Decapod 4**						x			0.05
		Decapod 5*		x	x		0.03				
		Decapod 6		x	x		0.13	x			0.01
Brachiopoda		Brachiopoda 1	i	x	x		8.85	x			0.53
Chordata	Ascidiacea	Ascidiacea 1*		x			0.08				
	Holocephali	***Chimaera monstrosa* (Linnaeus, 1758)**		x			0.01		x		0.02
	Actinopterygii	***Sebastes viviparus* (Krøyer, 1845)****	v						x		0.02
		Coryphaenoides rupestris* (Gunnerus, 1765)*						x			0.01
	Undetermined	**Pisces 1***		x			0.01				
		Pisces 2*			x		0.01				
		Pisces 3**	x							x	0.01
		Pisces 4**								x	0.02
Cnidaria	Hexacorallia*	*Bolocera tuediae* (Johnston, 1832)		x	x		0.34	x	x		0.18
		Sagartia sp.	k	x	x		0.86	x			0.75
		Protanthea simplex* (Carlgren, 1891)*						x			0.01
		Actiniaria 1	h, s	x	x	x	0.35		x		0.07
		Actiniaria 2*		x			0.11				
		Actiniaria 3**						x	x		0.84
		Actiniaria 4**						x			0.04
		Actiniaria 5**								x	0.05
		Actiniaria 6**						x			0.12
	Octocorallia*	*Anthomastus grandiflorus* (Verrill, 1878)	b	x			0.29	x			0.34
		Kophobelemnon stelliferum (Müller, 1776)	q	x			0.08	x	x		0.03
		Virgularia mirabilis* (Müller, 1776)	r	x			0.01				
		Octocorallia 1**						x			0.02
		Octocorallia 2**						x			0.02
		Octocorallia 3*		x			0.02				
Echinodermata	Asteroidea	*Ctenodiscus crispatus* (Bruzelius, 1805)*		x	x	x	0.04				
		Henricia spp.		x	x	x	0.06	x	x	x	0.44
		Hymenodiscus coronata (Sars, 1871)	o	x			0.17	x			0.34

(Continued)

TABLE 2 | Continued

				D1				D2			
Phylum	***Class (subclass*)***	***Taxon***	**Figure 4 *plate #***	***Basin***	***Intermediate***	***Above sill***	***Total %***	***Basin***	***Intermediate***	***Above sill***	***Total %***
		Poraniomorpha (Poraniomorpha) hispida* (M. Sars, 1872)*	f					x			0.01
		Pseudarchaster parellii (Düben & Koren, 1846)**							x	x	0.07
		Psilaster andromeda (Müller & Troschel, 1842)		x	x		0.04	x			0.01
		Pteraster militaris (O.F. Müller, 1776)		x	x	x	0.15	x	x	x	0.09
		Pteraster* sp.*						x			0.01
		Asteroidea 1	c	x			0.02	x			0.02
		Asteroidea 2**						x	x		0.02
		Asteroidea 3	i	x			0.01	x			0.02
		Asteroidea 4				x	0.01	x	x		0.02
		Asteroidea 5**						x		x	0.02
	Echinoidea	*Gracilechinus acutus* (Lamarck, 1816)	t, v, y	x	x	x	2.30	x	x	x	5.62
		Gracilechinus elegans (Düben & Koren, 1844)	s, x	x	x	x	1.83	x	x	x	1.26
		Echinoidea 1**	u					x	x	x	21.35
	Holothuroidea	*Bathyplotes natans* (M. Sars, 1868)		x			0.48	x			0.06
		Mesothuria intestinalis (Ascanius, 1805)		x	x		0.53	x			0.14
		Parastichopus tremulus (Gunnerus, 1767)	l, p, y	x	x	x	0.54	x	x	x	0.67
		Psolus squamatus (O.F. Müller, 1776)	e, j, m	x	x	x	23.09	x	x	x	19.31
	Ophiuroidea	*Ophiura albida* (Forbes, 1839)	g	x			0.02	x			0.03
		Ophiuroidea 1		x	x		0.37	x	x		0.18
		Ophiuroidea 2*		x			0.01				
		Ophiuroidea 3		x			0.01	x			0.01
Mollusca	Bivalvia	*Acesta excavata* (Fabricius, 1779)	d	x			0.11	x			1.27
	Polyplacophora	Polyplacophora 1*		x			0.01				
		Polyplacophora 2**						x			0.01
Porifera	Demospongiae	*Axinella infundibuliformis* (Linnaeus, 1759)	f	x		x	0.22	x	x		0.24
		Axinella rugosa (Bowerbank, 1866)		x	x		0.16	x			0.08
		Haliclona (Haliclona) urceolus (Rathke & Vahl, 1806)	t	x	x		0.90	x			0.25
		Hexadella dedritifera (Topsent, 1913)	g	x		x	0.01	x	x		0.84
		Hymedesmia sp.	g	x	x	x	11.34	x	x	x	7.98
		Phakellia ventilabrum (Linnaeus, 1767)	x	x	x	x	0.62	x	x		0.13
		Phakellia spp.	s, w	x	x	x	0.50	x			1.06
		Polymastia nivea (Hansen, 1885)		x	x	x	2.14	x	x		0.59
		Stryphnus fortis* (Vosmaer, 1885)		x			0.01				
		Stylocordyla borealis (Lovén, 1868)		x	x		0.97	X			0.14
		Thenea sp.*		x			0.02				
		Carnivorous Sponge 1*		x			0.04				
	Hexactinellida	*Asconema* aff. *foliatum* (Fristedt, 1887)	e	x			0.01	x			0.04
	Undetermined	**Orange Encrusting Sponge 1****						x			0.03
		White Encrusting Sponge 1	b, g	x	x	x	32.21	x	x	x	26.66
		Yellow Encrusting Sponge 1	g	x	x	x	1.48	x	x	x	2.26

(Continued)

TABLE 2 | Continued

				D1				D2			
Phylum	***Class (subclass*)***	***Taxon***	**Figure 4 *plate #***	***Basin***	***Intermediate***	***Above sill***	***Total %***	***Basin***	***Intermediate***	***Above sill***	***Total %***
		Brown Globular Sponge 1		x	x		0.09		x		0.01
		White Globular Sponge 1		x	x		0.17	x			0.06
		White Globular Sponge 2		x			0.03	x			0.03
		White Globular Sponge 3**						x			0.14
		Infundibuliform Sponge 1		x			0.02	x			0.02
		Infundibuliform Sponge 2		x	x		0.41	x			0.14
		Infundibuliform Sponge 3		x	x		0.03	x			0.03
		Infundibuliform Sponge 4**						x			0.01
		White Massive Sponge 1		x	x	x	0.72		x		0.03
		White Massive Sponge 2		x			0.12	x			0.05
		White Massive Sponge 3**						x			0.05
		Yellow Massive Sponge 1**						x			0.04
		Stalked Sponge 1		x	x		0.73	x			0.11
		White Verrucose Sponge 1**	a					x			0.08
		Indet Sponge 1*			x		0.01				
		Indet Sponge 2*		x			0.02				
		Indet Sponge 3*		x			0.02				
		Indet Sponge 4*		x			0.01				
Other		Unidentified 1*		x			0.13				
		Unidentified 2		x			0.04	x			0.01
		Unidentified 3		x		x	0.07	x			0.03
		Unidentified 4*		x			0.07				
		Unidentified 5*		x	x		0.54				
		Unidentified 6		x			0.05	x			0.31
		Unidentified 7**						x			0.14
		Unidentified 8**						x			0.06
		Unidentified 9*		x			0.01				
		Unidentified 10*		x			0.02				
		Unidentified 11*		x		x	0.03				
		Unidentified 12**						x			0.01
		Unidentified 13**						x			0.03
		Unidentified 14**						x			0.01
		Unidentified 15**						x			0.02
		Unidentified 16**						x			0.01
		Total abundance		9676	1449	432	11557	6837	3191	587	10615
		Total number of species		76	37	21	79	79	28	15	89
		Total number of images		275	32	13	320	165	18	8	191

*Total percentage (%) is the percentage of total abundance for each respective taxon. Asterisks denotes morphotaxa that were only observed within one dive, where * = Dive 1 and ** = Dive 2. Highlighted taxa are rare (<3 individuals) and dropped from statistical analyses.* ***Figure 4*** *plate reference indicates which* ***Figure 4*** *image plate that particular taxa can be found within. Bolded taxa are rare (<3 individuals) and dropped from statistical analyses.*

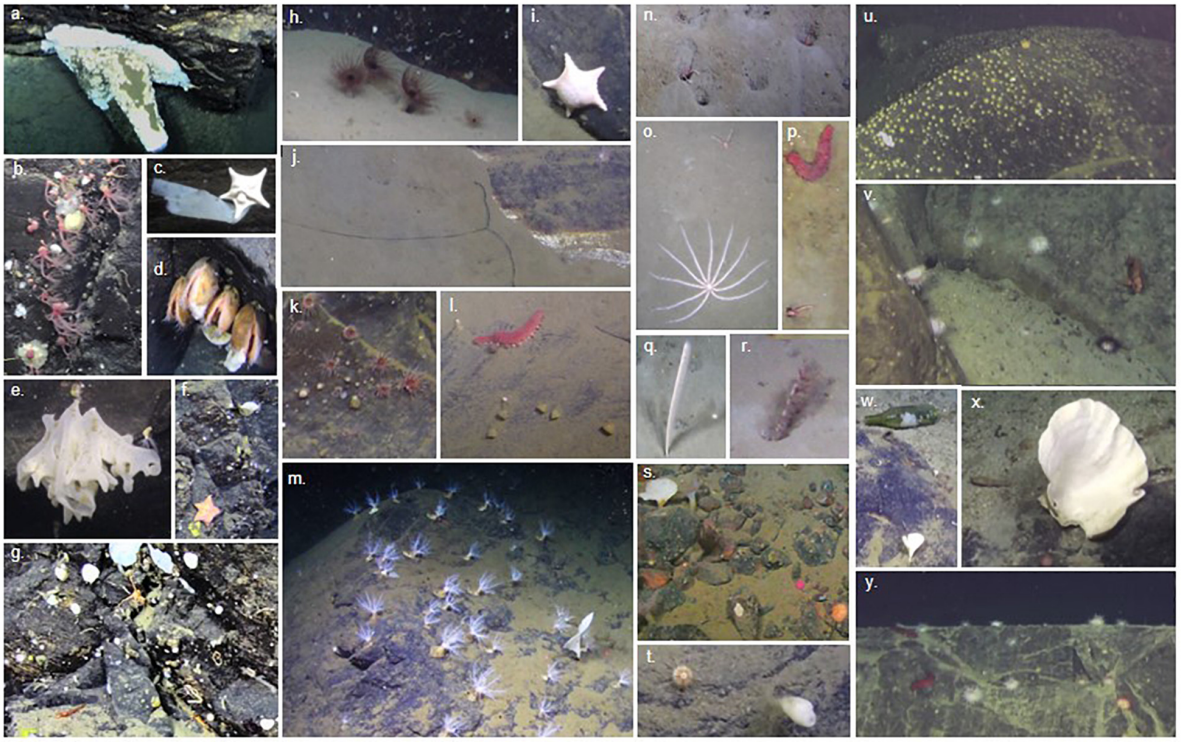

FIGURE 4 | Example of taxa and megafauna communities observed in Sognefjord, Norway. Panels **(a–g)** represents Basin Zone taxa on exposed hard substrate. Panels **(h–m)** displays Basin taxa in environments with both hard and soft substrate present. Panels **(n–r)** shows taxa common in soft sediment habitats. Panels **(s–u)** displays taxa within the Intermediate Zone. Panels **(v–y)** shows the Above Sill Zone. Refer to **Table 2** for the taxa identifications.

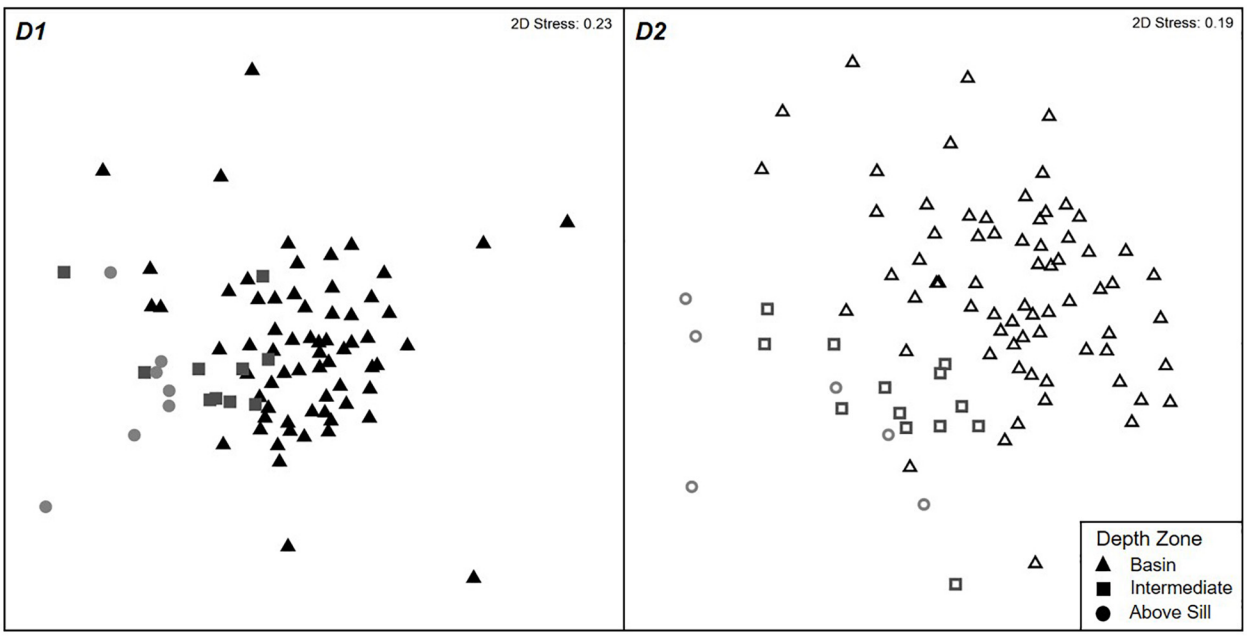

FIGURE 5 | Non-metric MDS ordination plots visualizing the Sørensen resemblances of the megafauna presence-absence data at different depth zones between Dive 1 (stress = 0.23; left) and Dive 2 (stress = 0.19; right). The distance between the points relates to the similarity of community composition at each depth, whereby the closer the points the more similar the community.

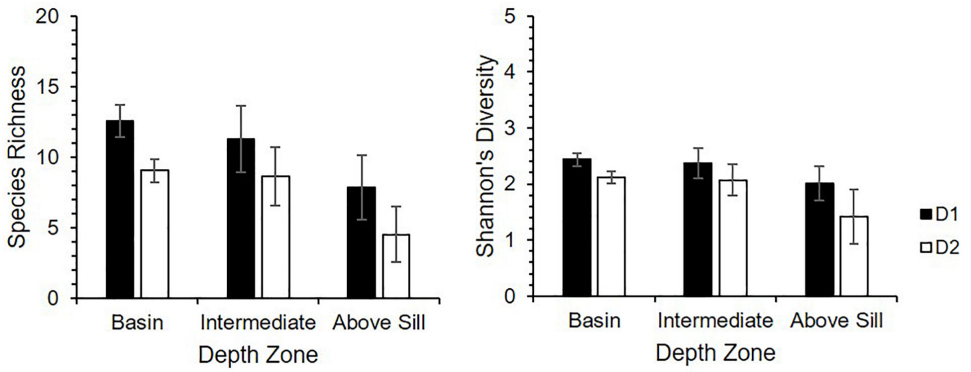

FIGURE 6 | Averaged diversity indices (species richness and Shannon-Wiener diversity index) per depth zone of the Dive 1 (D1; closed) and Dive 2 (D2; open) presence-absence community data in relation to the three depth zones in Sognefjord, Norway. Error bars represent 95% confidence intervals.

Zones had the largest difference in community composition (SIMPER, D1: Average dissimilarity = 63.03%; D2: Average dissimilarity = 78.87%). *Munida tenuimana*, *Parastichopus tremulus* (Gunnerus, 1767), Brachiopoda 1, *G. elegans*, and *Pteraster militaris* (O.F. Müller, 1776) contributed most to the differences between the Basin and Above Sill communities for D1. For D2, *M. tenuimana*, *P. squamatus*, *G. acutus*, *Hymedesmia* sp., and White Encrusting Sponge 1 contributed most to the differences between the two zones.

Diversity of Sognefjord's Megafauna Community

The diversity indices for the D2 (near-sill) zones were consistently lower than those of the corresponding zones in D1 (central) (**Figure 6**). For both dives, the diversity indices for the Above Sill Zones were lower than those of the deeper zones. The diversity indices all passed the Levene's test of homogeneity ($p > 0.05$), and the one-way ANOVA indicated that there were significant differences ($p < 0.001$) in the indices for D1 and D2 and their respective depth zones. The species richness and diversity were statistically significantly different between the D1 and D2 respective Basin Zones (Tukey HSD: $p < 0.01$). There was a significant difference in species richness between the Basin and Above Sill Zones for D1 (Tukey HSD: $p = 0.03$) and trend toward significant difference between the Basin and Above Sill Zones for D2 (Tukey HSD: $p = 0.069$). For the Shannon-Wiener diversity index, there was a significant difference between the Basin and Above Sill Zones for D2 (Tukey HSD: $p = 0.005$), and a significant difference between the Intermediate and Above Sill Zones (Tukey HSD: $p = 0.047$).

Environmental Influence on the Megafauna Community

Salinity and dissolved oxygen were the most influential variables on the diversity indices when considered separately, as revealed by GLMs (**Table 4** and **Supplementary Figure S3**), and depth had little influence alone. For species richness, the combination of depth and dissolved oxygen explained 10.85% of the deviance within the dataset. For diversity, the combination of depth, salinity, and dissolved oxygen explained 19.01% of the deviance in the dataset.

DISCUSSION

The present study provides a more recent overview of the Sognefjord megabenthic community composition than Bernd (1993) and focuses on the abiotic conditions more than was recently published by Buhl-Mortensen et al. (2017, 2020). The observations were similar to the findings from Bernd, where the deeper regions were characterized by sponges, holothurians and *Munida tenuimana*; however, in addition to sponges and holothurians, the shallower regions, particularly above the sill, had a higher abundance of urchins and anemones present.

Sognefjord shares some of the same fauna elements found in Hardangerfjord (Buhl-Mortensen and Buhl-Mortensen, 2014; Buhl-Mortensen et al., 2020). Both fjords are dominated by *Munida* sp., *Parastichopus tremulus*, *Psolus squamatus*, and *Phakellia* species. However, as stated by Buhl-Mortensen et al. (2020), and as was observed in this study, many of the taxa observed in Sognefjord are not present in Hardangerfjord.

As is common for fjord systems, many of the taxa observed are continental slope or deep-water species. For example, *Anthomastus grandiflorus* (Verril, 1878), which is considered a deep-sea species with a distribution of 457–1760 m (Molodtsova et al., 2008), was observed in small clusters on vertical rock walls at depths below 540 m, and *Kophobelemnon stelliferum* and *Virgularia mirabilis* (Müller, 1776) were both observed in low quantities in soft bottom regions at depths below 630 and 500 m, respectively. *Coryphaenoides rupestris* was observed in the Basin Zone of D2, a deep-water fish that has been found to have isolated subpopulations within Sognefjord (Delaval et al., 2018). A peculiar finding was the presence of very large specimens (up to 140 cm long) of the hexactinellid (glass) sponge *Asconema* aff. *foliatum* on vertical cliffs below 800 m depth at both dive sites, representing a group of species normally confined to deep and cold waters on the outer shelf off Northern Norway, or along the Reykjanes or Arctic Mid-Ocean Ridges (e.g., Tabachnick and Menshenina, 2007; Maldonado et al., 2016; Roberts et al., 2018).

TABLE 3 | Taxa responsible for the differences in the top 10 highest contributing megafauna within each zone identified in the similarity percentage analysis (SIMPER) for Dive 1 (Left) and Dive 2 (Right).

D1	*Morphotaxa*	*Sim/SD*	*%*	*Cumulative %*	*D2*	*Morphotaxa*	*Sim/SD*	*%*	*Cumulative %*
	Basin								
	*Psolus squamatus**	**1.99**	15.3	15.3		*Psolus squamatus**	**1.64**	20.2	20.2
	White Encrusting Sponge 1*	**1.78**	13.7	29.0		White Encrusting Sponge 1*	1.39	18.0	38.2
	*Munida tenuimana**	**1.67**	13.3	42.3		*Hymedesmia* sp.*	1.42	17.6	55.7
	Hymedesmia sp.*	**1.68**	12.3	54.6		*Munida tenuimana**	1.15	17.3	73.0
	Brachiopoda 1	0.91	7.8	62.4		Yellow Encrusting Sponge 1*	0.53	5.2	78.2
	Yellow Encrusting Sponge 1*	0.65	4.5	67.0		*Phakellia* spp.*	0.47	4.4	82.6
	Phakellia spp.*	0.63	4.5	71.5		*Gracilechinus acutus*	0.38	3.7	86.3
	Stylocordyla borealis	0.60	4.1	75.5		*Parastichopus tremulus*	0.23	1.6	87.9
	Haliclona (Haliclona) urceolus	0.56	3.6	79.2		Decapod 1	0.26	1.5	89.5
	Polymastia nivea	0.49	3.0	82.2		*Gracilechinus elegans*	0.26	1.5	91.0
	Intermediate								
	*Psolus squamatus**	**4.48**	16.6	16.6		*Parastichopus tremulus*	**1.99**	18.8	18.8
	White Encrusting Sponge 1*	**4.48**	16.6	33.1		White Encrusting Sponge 1*	1.4	15.2	34.1
	*Gracilechinus elegans**	**1.76**	13.4	46.5		*Gracilechinus acutus**	1.08	13.4	47.4
	Hymedesmia sp.*	**1.92**	12.0	58.5		*Psolus squamatus**	1.08	12.9	60.3
	Yellow Encrusting Sponge 1*	1.25	9.0	67.5		*Bolocera tuediae*	0.88	10.9	71.3
	Phakellia spp.	0.91	7.0	74.5		*Gracilechinus elegans**	0.87	9.7	81.0
	*Gracilechinus acutus**	0.91	6.8	81.3		*Hymedesmia* sp.*	0.73	6.8	87.7
	Polymastia nivea	0.69	4.8	86.1		Yellow Encrusting Sponge 1*	0.48	3.7	91.4
	Parastichopus tremulus	0.52	3.4	89.5		Echinoidea 1	0.36	3.5	94.9
	Haliclona (Haliclona) urceolus	0.53	3.2	92.6		Ophiuroidea 1	0.2	0.9	95.8
	Above Sill								
	White Encrusting Sponge 1*	**4.72**	23.4	23.4		*Gracilechinus acutus*	**3.55**	51.9	51.9
	Hymedesmia sp.*	**1.44**	16.0	39.4		Echinoidea 1	0.78	16.1	68.0
	*Parastichopus tremulus**	**1.46**	15.6	54.9		*Parastichopus tremulus**	0.46	12.7	80.7
	Gracilechinus elegans	**1.46**	15.6	70.5		Actiniaria 5	0.48	7.8	88.5
	Psolus squamatus	0.91	9.8	80.3		*Henricia* spp.	0.26	4.2	92.7
	Pteraster militaris	0.61	5.9	86.2		White Encrusting Sponge 1*	0.26	2.7	95.3
	Yellow Encrusting Sponge 1*	0.61	5.9	92.1		Yellow Encrusting Sponge 1*	0.26	2.4	97.8
	Phakellia spp.	0.62	5.2	97.2		*Hymedesmia* sp.*	0.26	2.2	100.0
	White Massive Sponge 1	0.22	1.1	98.4					
	Polymastia nivea	0.22	0.8	99.2					

Bolded taxa have the highest similarity (SIM)/standard deviation values (< 1.5). Asterisks (*) indicate taxa that were present in the respective depth zone for both dives.

Now we address each of this study's objectives in turn.

Community Patterns With Depth and Distance From the Sill

In general, much of the same taxa composition was observed in both dives for depth zones below the sill depth. The largest difference in megabenthic community composition was found between the deepest and shallowest zones for both dives, and similar trends have been observed in other surveys (Starmans et al., 1999; Sswat et al., 2015; Molina et al., 2019). In the present study, the Basin Zone was characterized more by sessile fauna (e.g., *P. squamatus, Acesta excavata, Hymenodiscus coronata*, and sponges) and *M. tenuimana*, whereas the Above Sill Zone was more dominated by echinoderms and anemones.

Contrary to numerous fjord and shelf-based studies (Buhl-Mortensen and Høisaeter, 1993; Holte et al., 2004; Webb et al., 2009; Włodarska-Kowalczuk et al., 2012; Sswat et al., 2015; Gasbarro et al., 2018; Molina et al., 2019), we find that communities at the shallowest depths (Above Sill Zone) and in closer proximity to the sill (D2) have the lowest number of species and diversity. Buhl-Mortensen et al. (2017, 2020) observed a similar trend in relation to the proximity to sill, where the outer region in Sognefjord had lower species richness compared to the middle region (Buhl-Mortensen et al., 2017, 2020). However, Buhl-Mortensen et al. (2020) observed a trend of decreasing species richness with increasing depth, which was not observed in the present study. The trends observed in the present study are more consistent with shelf community patterns observed by Starmans et al. (1999), where shallower regions contained a lower number of highly abundant taxa than the deeper stations and diversity increased with increasing water depth. This reduction in species richness and diversity in D2 (near-sill) and the areas above the sill could be driven by changes in water mass characteristics or increased physical stress on the

TABLE 4 | Summary statistics of the generalized linear models (GLMs) fitted to species richness and Shannon-Wiener diversity (Poisson distribution, quasi-Poisson error).

Diversity index	*Variable*	*Explained deviance*	*Residual deviance*	*% Explained*	*Pr(>|t|)*
Total number of species	Null		320.65		
	Depth (m)	0.99	319.66	0.31	0.461
	Salinity (psu)	14.75	305.90	4.60	0.006
	Dissolved oxygen (mL L^{-1})	22.13	298.52	6.90	0.001
	Chlorophyll *a* concentration (μg L^{-1})	0.00	320.65	0.00	0.980
	Exposed hard substrate (%)	5.31	315.34	1.66	0.089
	Soft sediment (%)	2.43	318.22	0.76	0.245
	Silicon (μmol L^{-1})	1.43	319.22	0.45	1.245
	Phosphate (μmol L^{-1})	0.43	320.22	0.13	2.245
	Ammonium (μmol L^{-1})	−0.57	321.22	−0.18	3.245
	Nitrate (μmol L^{-1})	−1.57	322.22	−0.49	4.245
	Nitrogen dioxide (μmol L^{-1})	−2.57	323.22	−0.80	5.245
	Best combination				
	Depth + dissolved oxygen	34.78	285.87	10.85	
Shannon-Wiener diversity	Null		21.09		
	Depth (m)	0.08	21.01	0.38	0.396
	Salinity (psu)	0.98	20.11	4.65	0.003
	Dissolved oxygen (mL L^{-1}	1.05	20.03	4.99	0.002
	Chlorophyll *a* concentration (μg L^{-1})	0.00	21.08	0.01	0.865
	Exposed hard substrate (%)	0.41	20.68	1.95	0.056
	Soft sediment (%)	0.02	21.07	0.08	0.712
	Silicon (μmol L^{-1})	1.43	319.22	0.45	1.245
	Phosphate (μmol L^{-1})	0.43	320.22	0.13	2.245
	Ammonium (μmol L^{-1})	−0.57	321.22	−0.18	3.245
	Nitrate (μmol L^{-1})	−1.57	322.22	−0.49	4.245
	Nitrogen dioxide (μmol L^{-1})	−2.57	323.22	−0.80	5.245
	Best combination				
	Depth + salinity + dissolved oxygen	2.07	19.01	9.83	

Percentage (%) explained is the percentage of null deviance in the data explained by the model.

benthic communities as the environmental conditions become less stable (Starmans et al., 1999; Jones et al., 2007).

Influence of Water Mass Properties and Sill Depth

The basin waters of both dives were fairly homogeneous (Storesund et al., 2017) and likely contributed to the homogeneity observed in the species composition in the deeper regions. Water mass properties (e.g., temperature, salinity, dissolved oxygen) play a significant role in megabenthic community composition (Buhl-Mortensen and Høisaeter, 1993; Williams et al., 2010: Meyer et al., 2015), which appears to be the case for Sognefjord as well. The changes in species composition appear to gradually occur around the transition between the basin and intermediate water masses, which is at approximately 300 m (Storesund et al., 2017), and more clearly near the sill depth. Studies have shown that sills affect water mass dynamics in ways that are critical to the structuring of benthic communities (Strømgren, 1970; Rüggeberg et al., 2011).

As Buhl-Mortensen and Høisaeter (1993) stated, the environment in fjord basins is influenced by the sill depth. With shallow sills, organic matter becomes trapped within the inner fjord below the sill depth and is not flushed out readily by the adjacent coastal water (Klitgaard-Kristensen and Buhl-Mortensen, 1999). As such, it is possible that organic input from renewal events and terrestrial sources (e.g., rivers, runoff, snowmelt, etc.) accumulates and has longer residence times in fjord basins (relative to shallower waters), providing food and nutrients to the benthic fauna below the sill depth. In a recent study of the Sognefjord by Buhl-Mortensen et al. (2020), the authors observed continuous detritus cover on sloping bedrocks at depths greater than 400 m and terrestrial organic material mixed in with the basin's soft sediment. The observed higher species richness and presence of deposit-feeding holothurians (*Bathyplotes natans* and *Mesothuria intestinalis*) and suspension-feeding *Hymenodiscus coronata* in the Basin Zone's soft bottom regions indicate availability of organic matter to the basin floor (Roberts and Moore, 1997; Flach et al., 1998; Amaro et al., 2015).

The vertical-falling particulate matter along the rocky walls observed in D1 is likely an important food source for many of the filter- and suspension-feeders (e.g., encrusting sponges, *Asconema* aff. *foliatum*, encrusting polychaetes, and *Acesta exacta*) residing on the vertical rock walls or under overhangs. Areas of flow acceleration owing to irregular topography (e.g., ridges, peaks, and other elevated substrate) experience increased

particle fluxes and are also likely important for suspension feeders (e.g., *Psolus squamatus*, *Phakellia* spp., *Phakellia ventilabrum*, and *Axinella infundibuliformis*) (Flach et al., 1998; Buhl-Mortensen et al., 2020). As is common in fjord environments, it is likely that the quality of food is lower in the basin and inner fjord compared to regions nearer to the sill (Klitgaard-Kristensen and Buhl-Mortensen, 1999). However, the higher species richness and presence of suspension- and deposit-feeders within the basin suggests the fauna may be adapted to the low quality of food, or that this is compensated by the stability of the basin environment. It is clear that a more rigorous study should be conducted to quantify and assess the quality of the organic matter supplied to the basin communities.

Environmental Dynamics

Depth, salinity, and dissolved oxygen were highlighted as important variables for the diversity indices. Depth acts as a proxy for other factors and it is likely that parameters which were not accounted for in the present study (e.g., food availability, particulate organic matter, localized hydrodynamics, pollution) are also influencing the patterns observed (Jones et al., 2007; Webb et al., 2009; Williams et al., 2010). Dissolved oxygen and percentage cover of substrate type varied most between the two dives, both of which are known to be critical for many benthic habitats (Holte et al., 2005; Williams et al., 2010; Sswat et al., 2015). The availability of hard substrate is important for sessile invertebrates (Williams et al., 2010; Buhl-Mortensen et al., 2012), and in this study, regions with exposed hard substrate were often covered with sponges, serpulid worm tubes, bivalves, and holothurians, similar to observations made by Gasbarro et al. (2018). However, for the Sognefjord megafauna community, there was not much difference in diversity and species richness between percent cover of hard substrate, soft bottom or mixed substrates. Therefore, it is possible that other factors like environmental dynamics or food availability is driving the patterns observed.

The megafauna communities at the mouth of the fjord (D2) showed lower diversity and species richness compared to central fjord (D1) communities. The central fjord environment is more stable than that of the fjord mouth, which is subjected to greater temporal variability (Storesund et al., 2017) due to exchange with the coastal ocean. Differences between the two dives are likely to be largely a result of horizontal environmental gradients along the fjord set up by biogeochemical and physical processes. For example, dissolved oxygen concentrations at the interface between the basin and intermediate water and at the sill depth differed slightly between dives (**Supplementary Figure S1**), the water being more oxygenated toward the sill (D2) because of the influence of coastal water. Dissolved oxygen concentrations at these depths are likely diminished with distance up-fjord by diffusion to and entrainment of vertically adjacent, less oxygenated waters and by the cumulative effects of (bacterial) respiration with distance from the sill (Storesund et al., 2017).

Areas with high environmental disturbance are characterized by an increase in mobile species, decrease in sessile fauna, and overall lower diversity (Włodarska-Kowalczuk et al., 2005; Jones et al., 2006; Webb et al., 2009; Hughes et al., 2010; Włodarska-Kowalczuk et al., 2012), as was observed in D2 and regions above the sill depth. The higher turbidity observed in D2 may have impacted the fjord benthic communities. Sessile suspension-feeding invertebrates are at a risk of smothering in areas with high quantities of suspended material in the water column (Jones et al., 2006; Kutti et al., 2015; Meyer et al., 2015). Fauna that are not limited by such conditions can persist (Rygg, 1985; Włodarska-Kowalczuk et al., 2005, 2012; Gasbarro et al., 2018), sometimes in high abundances, which could contribute to the increased abundance of echinoderms and reduced occurrences of sponges and sessile holothurians in the shallower regions of the fjord. Buhl-Mortensen et al. (2020) also noted that the shallower and silled regions of the fjord have relatively strong currents, whereas, the bottom currents in the basin were weak. This supports the general picture of gradients in environmental variability and stress within the fjord.

Future Implications

The environmental conditions in Sognefjord are affected by anthropogenic influences, such as cruise ships, fish farms, hydroelectric stations, and pollution (Manzetti and Stenersen, 2010). There is limited information concerning how such influences impact the Sognefjord community, though fish stocks have seen a considerable reduction (see Manzetti and Stenersen, 2010) and the shellfish community showed increased diarrhetic shellfish poisoning toxins with increased distance into the fjord (Ramstad et al., 2001).

A study by Rygg (1985) found that fjords with high pollutant concentrations were characterized by opportunistic species. Additional organic input from anthropogenic sources like fish farming or nutrient runoff may lead to hypoxic conditions in the fjord basin (Levin et al., 2009; Johansen et al., 2018). Johansen et al. (2018) predicted that increased organic matter within Norwegian fjord basins will lead to a dominance of deposit feeders, while the presence of suspension feeders will decline. Similar to the findings of Rygg (1985), Johansen et al. (2018) also found a shift in the community structure toward opportunistic species as a result of oxygen depletion and increased temperatures. Coastal water temperatures have been rising (Aure, 2016), which has led to increased temperatures within fjord basins (Johansen et al., 2018), resulting in changes in stratification and reduced oxygen supply. Long-time series temperature and organic input data are not readily available for Sognefjord, but if its environmental conditions follow the trajectories of other Norwegian fjords it is possible to predict a similar shift toward more opportunistic species. The present study does not include any temporal replication and the impact and future implications of anthropogenic-derived environmental change on the system is largely unknown and requires more research.

CONCLUSION

This study provides a recent overview of Sognefjord's megabenthic community near the sill of the fjord and the central fjord. Megafauna community composition was homogeneous within the fjord basin; however, species richness and diversity declined with proximity to the sill and with decreasing

water depth, particularly at the boundary between basin and intermediate water and at the sill depth. The fjord basin was characterized by *Psolus squamatus*, *Munida tenuimana*, *Phakellia* sp., *Acesta excavata*, and encrusting sponges. At shallower depths, the fjord was dominated by echinoderms, particularly in the dive closest to the sill. It is clear that more research is needed to understand the influence of shallow sills and water mass structure on fjord communities, as this study shows these features are important to Sognefjord's megabenthic communities. The clear stratification occurring between the basin water and intermediate water within Sognefjord would make it well suited for future surveys designed to monitor a wider range of environmental conditions or to understand future scenarios with stratification changes or deoxygenation.

DATA AVAILABILITY STATEMENT

The datasets generated for this study can be found at PANGAEA: https://doi.pangaea.de/10.1594/PANGAEA.914801.

AUTHOR CONTRIBUTIONS

HR, ER, and FM collected the video footage, CTD casts, and nutrient data for the study. HM annotated the video footage. HR provided fauna identifications. ER interpreted the *in situ* abiotic conditions and calculated the slope and distance from the sill for the transects. HM performed the statistical analysis. FM provided the sampling design, analysis and description for the nutrient contents. HM wrote the manuscript. All the authors read, edited, and approved the final manuscript.

FUNDING

The work leading to this publication has received funding from the European Union's Horizon 2020 Research and Innovation Programme through the SponGES project (Grant Agreement No. 679849). This document reflects only the authors' view and the Executive Agency for Small and Medium-sized Enterprises (EASME) is not responsible for any use that may be made of the information it contains. FM is supported by the Innovational Research Incentives Scheme of the Netherlands Organisation for Scientific Research (NWOVIDI Grant No. 016.161.360).

ACKNOWLEDGMENTS

The video footage and CTD casts were collected in 2017 on the RV *G.O. Sars* during a SponGES cruise, therefore, the crew of the RV *G.O. Sars* and the ROV *AEgir 6000* as well as participating SponGES team are thanked for their contribution to this project. EMODnet Bathymetry Consortium (2018) is acknowledged for the use of high-resolution bathymetry map for Sognefjord. The work presented here is dedicated to the memory of our friend and mentor HR, who spent his life improving global understanding of deep-sea sponges.

SUPPLEMENTARY MATERIAL

The Supplementary Material for this article can be found online at: https://www.frontiersin.org/articles/10.3389/fmars.2020.00393/full#supplementary-material

REFERENCES

Amaro, T., de Stigter, H., Lavaleye, M., and Duineveld, G. (2015). Organic matter enrichment in the whittard channel; its origin and possible effects on benthic megafauna. *Deep Sea Res. Part I Oceanogr. Res. Pap.* 102, 90–100. doi: 10.1016/j.dsr.2015.04.014

Aure, J. (2016). *Kystklima. Havforskningsrapporten-2016. Fisken Havet Særnummer 1-2016*. Bergen: Institute of Marine Research.

Bernd, C. (1993). A television and photographic survey of megafaunal abundance in Central Sognefjorden, Western Norway. *Sarsia* 78, 1–8. doi: 10.1080/00364827.1993.10413515

Blanchard, A. L., Feder, H. M., and Hoberg, M. K. (2010). Temporal variability of benthic communities in an Alaskan glacial fjord, 1971-2007. *Mar. Environ. Res.* 69, 95–107. doi: 10.1016/j.marenvres.2009.08.005

Buhl-Mortensen, L., Buhl-Mortensen, P., Dolan, M. F. J., Dannheim, J., Bellec, V., and Holte, B. (2012). Habitat complexity and bottom fauna composition at different scales on the continental shelf and slope of northern Norway. *Hydrobiologia* 685, 191–219. doi: 10.1007/s10750-011-0988-986

Buhl-Mortensen, L., Buhl-Mortensen, P., Glenner, H., and Båmstedt, U. (2017). Dyphavshabitater langt inn i landet: nye undersøkelser av havbunnen i sognefjorden. *Naturen* 6, 246–251.

Buhl-Mortensen, L., Buhl-Mortensen, P., Glenner, H., Båmstedt, U., and Bakkeplass, K. (2020). Chapter 19 -The inland deep sea - benthic biotopes in the Sognefjord. *Seafloor Geomorphol. Benthic Habit.* 5, 355–372. doi: 10.1016/B978-0-12-814960-7.00019-11

Buhl-Mortensen, L., and Høisaeter, T. (1993). Mollusc fauna along an offshore-fjord gradient. *Mar. Ecol. Prog. Ser.* 97, 209–224. doi: 10.3354/meps097209

Buhl-Mortensen, P., and Buhl-Mortensen, L. (2014). Diverse and vulnerable deep-water biotopes in the Hardangerfjord. *Mar. Biol. Res.* 10, 253–273. doi: 10.1080/17451000.2013.810759

Delaval, A., Dahle, G., Knutsen, H., Devine, J., and Salvanes, A. G. V. (2018). Norwegian fjords contain sub-populations of roundnose grenadier, Coryphaenoides rupestris, a deep-water fish. *Mar. Ecol. Prog. Ser.* 586, 181–192. doi: 10.3354/meps12400

Drewnik, A., Wêsławski, J. M., Włodarska-Kowalczuk, M., Łącka, M., Promińska, A., Zaborska, A., et al. (2016). From the worm's point of view. I: environmental settings of benthic ecosystems in Arctic fjord (Hornsund, Spitsbergen). *Polar Biol.* 39, 1411–1424. doi: 10.1007/s00300-015-1867-1869

EMODnet Bathymetry Consortium (2018). *EMODnet Digital Bathymetry (2018).* Available online at: https://www.emodnet-bathymetry.eu/data-products/acknowledgement-in-publications

Environmental Systems Research Institute [ESRI], (2016). *ArcGIS Release 10.4*. Redlands, CA: ESRI.

Flach, E., Lavaleye, M., de Stigter, H., and Thomsen, L. (1998). Feeding types of benthic community and particle transport across the N.W. European continental margin (Goban Spur). *Prog. Oceanogr.* 42, 209–231. doi: 10.1016/S0079-6611(98)00035-34

Gasbarro, R., Wan, D., and Tunnicliffe, V. (2018). Composition and functional diversity of macrofaunal assemblages on vertical walls of a deep northeast Pacific fjord. *Mar. Ecol. Prog. Ser.* 597, 47–64. doi: 10.3354/meps12599

Grasshoff, K., Erhardt, M., and Kremling, K. V. (1983). *Methods of Seawater Analysis*. Weinheim: John Wiley & Sons.

Helder, W., and De Vries, R. T. P. (1979). An automatic phenol-hypochlorite method for determination of ammonia in sea- and brackish waters. *Neth. J. Sea Res.* 13, 154–160. doi: 10.1016/0077-7579(79)90038-90033

Holte, B., Oug, E., and Cochrane, S. (2004). Depth-related benthic macrofaunal biodiversity patterns in three undisturbed north Norwegian fjords. *Sarsia* 89, 91–101. doi: 10.1080/00364820410003496

Holte, B., Oug, E., and Dahle, S. (2005). Soft-bottom fauna and oxygen minima in sub-arctic north Norwegian sill basins. *Mar. Biol. Res.* 1, 85–96. doi: 10.1080/17451000510019033

Hughes, S. J. M., Jones, D. O. B., Hauton, C., Gates, A. R., and Hawkins, L. E. (2010). An assessment of drilling disturbance on *Echinus acutus* var. *norvegicus* based on in-situ observations and experiments using a remotely operated vehicle (ROV). *J. Exp. Mar. Bio. Ecol.* 395, 37–47. doi: 10.1016/j.jembe.2010.08.012

Jantzen, C., Haussermann, V., Forsterra, G., Laudien, J., Ardelan, M., Maier, S., et al. (2013). Occurrence of a cold-water coral along natural pH gradients (Patagonia, Chile). *Mar. Biol.* 160, 2597–2607. doi: 10.1007/s00227-013-2254-2250

Johansen, P.-O., Isaksen, T. E., Bye-Ingebrigtsen, E., Haave, M., Dahlgren, T. G., Kvalø, S. E., et al. (2018). Temporal changes in benthic macrofauna on the west coast of Norway resulting from human activities. *Mar. Pollut. Bull.* 128, 483–495. doi: 10.1016/j.marpolbul.2018.01.063

Jones, D. O. B., Bett, B. J., and Tyler, P. A. (2007). Depth-related changes in the arctic epibenthic megafaunal assemblages of Kangerdlugssuaq, East Greenland. *Mar. Biol. Res.* 3, 191–204. doi: 10.1080/17451000701455287

Jones, D. O. B., Hudson, I. R., and Bett, B. J. (2006). Effects of physical disturbance on the cold-water megafaunal communities of the Faroe-Shetland Channel. *Mar. Ecol. Prog. Ser.* 319, 43–54. doi: 10.3354/meps319043

Klitgaard-Kristensen, D., and Buhl-Mortensen, L. (1999). Benthic foraminifera along an offs.hore-fjord gradient: a comparison with amphipods and molluscs. *J. Nat. Hist.* 33, 317–350. doi: 10.1080/002229399300281

Kutti, T., Bannister, R. J., Fossa, J. H., Krogness, C. M., Tjensvoll, I., and Sovik, G. (2015). Metabolic responses of the deep-water sponge *Geodia barretti* to suspended bottom sediment, simulated mine tailings and drill cuttings. *J. Exp. Mar. Biol. Ecol.* 473, 64–72. doi: 10.1016/j.jembe.2015.07.017

Levin, L. A., Ekau, W., Gooday, A. J., Jorissen, F., Middelburg, J. J., Naqvi, S. W. A., et al. (2009). Effects of natural and human-induced hypoxia on coastal benthos. *Biogeosciences* 6, 2063–2098. doi: 10.5194/bg-6-2063-2009

Maldonado, M., Aguilar, R., Bannister, R. J., Bell, J. J., Conway, K. W., Dayton, P. K., et al. (2016). "Sponge grounds as key marine habitats: a synthetic review of types, structure, functional roles, and conservation concerns," in *Marine Animal Forests: the Ecology of Benthic Biodiversity Hotspots*, eds S. Rossi, L. Bramanti, A. Gori, and C. Orejas. (Springer: Switzerland), 1–39.

Manzetti, S., and Stenersen, J. H. V. (2010). A critical view of the environmental condition of the Sognefjord. *Mar. Pollut. Bull.* 60, 2167–2174. doi: 10.1016/j.marpolbul.2010.09.019

Meyer, K. S., Sweetman, A. K., Young, C. M., and Renaud, P. E. (2015). Environmental factors structuring Arctic megabenthos – a case study from a shelf and two fjords. *Front. Mar. Sci.* 2:22. doi: 10.3389/fmars.2015.00022

Molina, E. J., Silberberger, M. J., Kokarev, V., and Reiss, H. (2019). Environmental drivers of benthic community structure in a deep sub-arctic fjord system. *Estuar. Coast. Shelf Sci.* 225:106239. doi: 10.1016/j.ecss.2019.05.021

Molodtsova, T. N., Sanamyan, N. P., and Keller, N. B. (2008). Anthozoa from the northern mid-atlantic ridge and charlie-gibbs fracture zone. *Mar. Biol. Res.* 4, 112–130. doi: 10.1080/17451000701821744

Murphy, J., and Riley, J. P. (1962). A modified single solution method for the determination of phosphate in natural waters. *Anal. Chim. Acta* 27, 31–36. doi: 10.1016/S0003-2670(00)88444-88445

Poremba, K., and Jeskulke, K. (1995). Microbial activity in the sediment of the Sognefjord (Norway). Helgoländ. Meeresuntersuchun. 49, 169-176.

RStudio Team (2019). *RStudio: Integrated Development.* Boston: R. RStudio, Inc. Available online at: http://www.rstudio.com/

Ramstad, H., Hovgaard, P., Yasumoto, T., Larsen, S., and Aune, T. (2001). Monthly variations in diarrhetic toxins and yessotoxin in shellfish from coast to inner part of the Sognefjord, Norway. *Toxicon.* 39, 1035–1043. doi: 10.1016/S0041-0101(00)00243-249

Renaud, P. E., Włodarska-Kowalczuk, M., Trannum, H., Holte, B., Wêsławski, J. M., Cochrane, S., et al. (2007). Multidecadal stability of benthic community structure in a high-Arctic glacial fjord (van Mijenfjord, Spitsbergen). *Polar Biol.* 30, 295–305. doi: 10.1007/s00300-006-0183-189

Roberts, D., and Moore, H. M. (1997). Tentacular diversity in deep-sea deposit-feeding holothurians: implications for biodiversity in the deep sea. *Biodivers. Conserv.* 6, 1487–1505. doi: 10.2307/1543510

Roberts, E. M., Mienis, F., Rapp, H. T., Hanz, U., Meyer, H. K., and Davies, A. J. (2018). Oceanographic setting and short-timescale environmental variability at an Arctic seamount sponge ground. *Deep Sea Res. Part I Oceanogr. Res. Pap.* 138, 98–113. doi: 10.1016/j.dsr.2018.06.007

Rüggeberg, A., Flögel, S., Dullo, W.-C., Hissmann, K., and Freiwald, A. (2011). Water mass characteristics and sill dynamics in a subpolar cold-water coral reef setting at Stjernsund, northern Norway. *Mar. Geol.* 282, 5–12. doi: 10.1016/j.margeo.2010.05.009

Rygg, B. (1985). Distribution of species along pollution-induced diversity gradients in benthic communities in Norwegian fjords. *Mar. Pollut. Bull.* 16, 469–474. doi: 10.1016/0025-326X(85)90378-90379

Sswat, M., Gulliksen, B., Menn, I., Sweetman, A. K., and Piepenburg, D. (2015). Distribution and composition of the epibenthic megafauna north of Svalbard (Arctic). *Polar Biol.* 38, 861–877. doi: 10.1007/s00300-015-1645-1648

Starmans, A., Gutt, J., and Arntz, W. E. (1999). Mega-epibenthic communities in Arctic and Antarctic shelf areas. *Mar. Biol.* 135, 269–280. doi: 10.1007/s002270050624

Storesund, J. E., Sandaa, R. A., Thingstad, T. F., Asplin, L., Albretsen, J., and Erga, S. R. (2017). Linking bacterial community structure to advection and environmental impact along a coast-fjord gradient of the Sognefjord, western Norway. *Prog. Oceanogr.* 159, 13–30. doi: 10.1016/j.pocean.2017.09.002

Strickland, J. D. H., and Parsons, T. R. (1968). A practical handbook of seawater analysis. *Bull. Fish. Res. Board Canada* 167, 1–31.

Strømgren, T. (1970). Emergence of *Paramuricea placomus* (L.) and *Primnoa resedaeformis* (Gunn.) in the inner part of *Trondheimsfjord* (West coast of Norway). *K. Norske Vidensk. Selsk. Skr.* 70, 1–5.

Svendsen, S. W. (2006). *Stratification and Circulation in Sognefjorden*. Master's thesis, University of Bergen, Bergen.

Sweetman, A. K., and Witte, U. (2008). Macrofaunal response to phytodetritus in a bathyal Norwegian fjord. *Deep Sea Res. Part I Oceanogr. Res. Pap.* 55, 1503–1514. doi: 10.1016/j.dsr.2008.06.004

Tabachnick, K. R., and Menshenina, L. L. (2007). Revision of the genus *Asconema* (Porifera : Hexactinellida : Rossellidae). *J. Mar. Biol. Assoc. U. K.* 87, 1403–1429.

Webb, K. E., Barnes, D. K. A., and Gray, J. S. (2009). Benthic ecology of pockmarks in the Inner Oslofjord, Norway. *Mar. Ecol. Prog. Ser.* 387, 15–25. doi: 10.3354/meps08079

Wei, T., and Simko, V. (2017). *R Package "Corrplot": Visualization of a Correlation Matrix (Version 0.84)*. Available online at: https://github.com/taiyun/corrplot

Williams, A., Althaus, F., Dunstan, P. K., Poore, G. C. B., Bax, N. J., Kloser, R. J., et al. (2010). Scales of habitat heterogeneity and megabenthos biodiversity on an extensive Australian continental margin (100-1100-m depths). *Mar. Ecol.* 31, 222–236. doi: 10.1111/j.1439-0485.2009.00355.x

Witte, U., Aberle, N., Sand, M., and Wenzhöfer, F. (2003). Rapid response of a deep-sea benthic community to POM enrichment: an in situ experimental study. *Mar. Ecol. Prog. Ser.* 251, 27–36. doi: 10.3354/meps251027

Włodarska-Kowalczuk, M., and Pearson, T. H. (2004). Soft-bottom macrobenthic faunal associations and factors affecting species distributions in an Arctic glacial fjord (Kongsfjord, Spitsbergen). *Polar Biol.* 27, 155–167. doi: 10.1007/s00300-003-0568-y

Włodarska-Kowalczuk, M., Pearson, T. H., and Kendall, M. A. (2005). Benthic response to chronic natural physical disturbance by glacial sedimentation in an Arctic fjord. *Mar. Ecol. Prog. Ser.* 303, 31–41.

Włodarska-Kowalczuk, M., Renaud, P. E., W?sławski, J. M., Cochrane, S. K. J., and Denisenko, S. G. (2012). Species diversity, functional complexity and rarity in Arctic fjordic versus open shelf benthic systems. *Mar. Ecol. Prog. Ser.* 463, 73–87. doi: 10.3354/meps09858

Zuur, A. F., Ieno, E. N., Walker, N. J., Saveliev, A. A., and Smith, G. M. (2009). *Mixed Effect Models and Extensions in Ecology with R. Statistics for Biology and Health*. New York, NY: Springer.

Conflict of Interest: The authors declare that the research was conducted in the absence of any commercial or financial relationships that could be construed as a potential conflict of interest.